Mechanical Technology and Engineering Insights

www.mtei.reapress.com

Mech. Technol. Eng. Insights. Vol. 3, No. 1 (2026) 39–55.

Paper Type: Original Article

Optimal Design of S-Shaped Energy Absorbers Using Radial Basis Function Neural Networks and Differential Evolution Algorithm

Ali Jamali[1,*], Fereshteh Poorahangryan[2], Sahar Hatami Pour[3]

[1] Department of Engineering, RMIT University, Melbourne, Australia; JAMALI.A@gmail.com.

[2] Department of Electrical Engineering, Ayandegan University, Tonekabon, Iran; f.ahangaryan@gmail.com.

[3] Department of Industrial Engineering, Ayandegan University, Tonekabon, Iran; saharhatamipour01@gmail.com.

Citation:

Received: 14 May 2025 *Revised: 23 July 2025* *Accepted: 26 August 2025*	Jamali, A., Poorahangryan, F., & Hatami Pour, S. (2026). Optimal design of s-shaped energy absorbers using radial basis function neural networks and differential evolution algorithm. *Mechanical Technology and Engineering Insights*, *3*(1), 39-55.

Abstract

The presented study introduces a multiobjective optimization approach that combines numerical and surrogate modeling approaches in order to enhance the crashworthiness characteristics of thin-walled S-shape energy absorbers under axial impact loading. In particular, the optimization problem includes the maximization of energy absorption and minimization of peak crushing force by changing four important geometrical variables such as cross-section width, curvature angle, curvature radius, and wall thickness. To conduct the simulation of the progressive crushing process with large deformation, local buckling, plastic folding, and self-contact phenomena, a 3D finite element model was developed using ABAQUS/explicit. These results have been verified against reference values, with the largest difference between theoretical and experimental values in relation to the absorbed energy and peak crushing force being equal to 2.86% and 0.75%, respectively. The database consisting of 58 absorbers was developed through numerical simulation. In turn, surrogate models based on Radial Basis Function (RBF) and Group Method of Data Handling (GMDH) were built from that database. It should be noted that GMDH showed excellent performance with determination coefficients equal to 0.9882 and 0.9725 for absorbed energy and peak crushing force, respectively. The developed surrogate models were later coupled with Differential Evolution (DE) to carry out the optimization analysis in order to construct the Pareto front. Eight non-dominated solutions were achieved, highlighting the natural trade-off between the energy absorption capacity and peak crushing force. Amongst the obtained solutions, one was selected as the compromise solution, which had an energy absorption of about 33,400 J and peak crushing force of about 8,713 N. The results reveal that the proposed integration of finite element modeling, neural-network surrogate model, and DE is quite effective in performing crashworthiness optimization of S-shaped energy absorber design at a significantly lower computational cost.

Keywords: S-shaped energy absorber, Crashworthiness, Multiobjective optimization, Radial basis function neural network, GMDH, Differential evolution, Finite element analysis, Pareto front.

1 | Introduction

The increase in speed and performance of vehicles in recent decades, along with the development of requirements for structural weight reduction, has heightened the importance of designing safety components and energy absorbers in transportation systems. During a collision, a significant portion of kinetic energy

Corresponding Author: JAMALI.A@gmail.com

https://doi.org/10.48313/mtei.v3i1.79

must be dissipated through the controlled deformation of structural components, in a manner that prevents excessive forces from being transmitted to occupants while also avoiding severe damage to the main vehicle components [1], [2]. Hence, the development of structures with high energy absorption capacity, along with controllable weight and crushing force, has become one of the most important topics in the field of impact-resistant structural design.

Various kinds of energy-absorbing elements can be found. However, thin-walled structures have drawn much interest because of their appropriate strength-to-weight ratio, easier manufacturing processes, and proper energy-absorbing capacity by means of bending, stretching, shearing, and buckling [1], [3]. The behavior of these structures under axial loading is typically accompanied by progressive folding and the conversion of kinetic energy into plastic deformation energy [2]. The performance of an energy absorber can be evaluated using indicators such as absorbed energy, peak crushing force, mean crushing force, and specific absorbed energy. In an optimal design, it is necessary to maximize the absorbed energy as much as possible, while keeping the peak crushing force within an acceptable range.

The majority of early studies on energy absorbers focused on straight tubes and straight thin-walled sections. Wierzbicki and Akerstrom [2], as well as Redwood [3], investigated the crushing behavior of thin-walled structures and studied the role of sequential buckling mechanisms in the energy absorption process. These studies provided a foundation for the development of analytical and numerical models of thin-walled structures under axial loading. Yamazaki and Han [4] used the response surface method and design of experiments to investigate the maximization of energy absorption in tubes. They demonstrated the importance of geometric parameters in determining energy absorber performance. Nariman-zadeh et al. [5] employed multiobjective genetic algorithms to optimize the energy absorption of square aluminum columns and showed the capability of evolutionary methods in solving multiobjective problems of energy absorbers. Zhang et al. [6] explored bitubular geometries employing surrogate models together with genetic algorithms. They showed that the combination of numerical simulation and optimization techniques can lower the cost associated with the design of energy-absorbing structures. Moreover, Zarei and Kröger [7], [8] found that the use of surrogate modeling helps considerably in reducing the cost of analysis because of the optimization of foam-filled tubes and honeycomb structures.

Although many studies have been conducted on straight structure optimization, in the actual automotive design process, due to lack of space, powertrain arrangement, and chassis shape, the application of curved structures cannot be avoided. Among these, S-shaped energy absorbers are of particular importance due to their adaptability to confined spaces and the ability to create suitable load paths. However, the mechanical behavior of these structures is far more complex than that of straight structures, because the simultaneous deformation caused by axial loading, bending, local buckling, and the geometric effects of curvature significantly influence the collapse pattern and force–displacement response [9], [10]. Therefore, simultaneously achieving high energy absorption capacity and controlled crushing force in S-shaped absorbers is a challenging problem in impact-resistant structural design.

Numerous experimental and numerical studies have been conducted on the behavior of curved and S-shaped structures. Ohkami et al. [9] investigated the collapse of thin-walled curved beams with closed hat-sections under various loading conditions and identified different collapse modes. Kim and Wierzbicki [11], [12] examined the effect of cross-sectional shape on the impact behavior of S-shaped structures. They showed that changes in cross-sectional geometry can significantly influence the deformation mechanism and energy absorption capability. Zheng and Wierzbicki [13] studied the quasi-static crushing behavior of an S-shaped aluminum front rail. They emphasized the importance of boundary conditions, specimen fixturing, and contact conditions in accurately predicting structural behavior. Zhang and Saigal [14] also investigated the impact behavior of a three-dimensional S-shaped space frame and demonstrated the complexity of the interaction between structural geometry and collapse mechanisms. To better understand the effect of cross-sectional parameters, Esmaeili-Marzdashti et al. [15] examined various cross-sections (triangular, square, hexagonal, and circular) in single-cell and multi-cell S-shaped structures. They showed that proper cross-section selection can significantly increase specific energy absorption. Soheili and Feli [16] recently studied the effects of grooves and cross-sectional shape on the energy absorption of S-shaped tubes under quasi-static and impact loading, demonstrating that smart grooves can control the peak crushing force without significantly reducing absorbed energy.

Focusing on the optimization of S-shaped energy absorbers, Han and Yamazaki [17] used the response surface method and the DOT optimization algorithm to optimize the performance of square S-shaped tubes. Their results showed that thickness modification in curved regions and appropriate geometric changes in straight sections can improve energy absorption capability. Liu et al. [18] used the sequential response surface method and numerical modeling in LS-DYNA software for optimizing the geometrical design of the S-frame. Their research has led to a remarkable improvement in the crushing efficiency of the S-frame. Nguyen et al. [19] applied a multiobjective particle swarm optimization algorithm on reinforced S-shaped frames subjected to axial dynamic loading. They showed that internal reinforcements can improve the specific energy absorption performance.

Hosseini-Tehrani and Nikahd [20] proposed a two-material approach for the S-shaped structure to improve strength indices and reduce weight. The optimization of the S-shaped front rail was carried out by Krzywobłocki [21] through the use of the macro-element technique and an evolutionary algorithm, where the computation cost is much less when compared to the FEA approach, proving that alternative techniques are efficient. The reliability-based robust optimization of an S-shaped energy absorber accounting for parametric uncertainties was described by Khalkhali et al. [22]. Yao et al. [23] proposed a Differential Evolution (DE)-based optimization method with weighted graph representation for subway underframe structures, which has the potential to be generalized to S-shaped energy absorbers.

A review of previous studies indicates that geometric parameters strongly influence the performance of S-shaped absorbers. Among the most important of these parameters are wall thickness, cross-sectional width, curvature radius, and curvature angle. Simultaneous changes in these parameters can significantly alter the collapse mechanism, absorbed energy, and crushing force. On the other hand, direct optimization of these parameters using finite element simulations, especially in multiobjective problems, requires a large number of numerical analyses and consequently considerable computational cost. Furthermore, the relationship between geometric variables and crashworthiness responses is usually complex due to the highly nonlinear nature of the collapse process, which limits the application of classical optimization methods [24], [25].

In recent years, the use of surrogate models based on artificial intelligence has received increasing attention as an effective solution to reduce the computational cost of engineering optimization problems. Artificial neural networks, due to their ability to approximate nonlinear and complex relationships between input and output variables, are well-suited for creating surrogate models of structural responses. Among various types of neural networks, the Radial Basis Function (RBF) neural network, due to its relatively simple structure, ability to approximate nonlinear relationships, and appropriate performance in engineering problems, can serve as an efficient tool for modeling the response of energy absorbers.

Sun et al. [26] demonstrated the efficiency of surrogate models in vehicle body design by combining the response surface method with multiobjective robust optimization. Fang et al. [27] also employed reliability-based optimization and surrogate models for the optimal design of vehicle components. Acar et al. [28] confirmed the key role of response surface models in reducing the number of simulations through multiobjective optimization of tapered tubes with axisymmetric indentations.

In very recent research, Homsnit et al. [29] used artificial neural networks for the optimization of automotive S-rail design. They showed that the ANN-based approach can extract the Pareto front with high accuracy and low computational cost. Gao et al. [30] proposed an active learning method for multiobjective optimization of thin-walled structures, in which surrogate models are adaptively updated, achieving high efficiency in finding optimal designs. Fengmin et al. [31] in 2025 used a stacked regression surrogate model for multiobjective optimization of lightweighting and crashworthiness of automotive front-end structures, significantly improving prediction accuracy.

Research in 2025 in the field of deep learning [32], [33] has also shown that frameworks based on deep neural networks and physics-informed surrogate models can enable high-accuracy rapid crashworthiness assessment. The combination of such surrogate models with evolutionary algorithms enables fast exploration of the design space and attainment of a set of optimal designs without the need for repeated expensive finite element analyses [34], [35].

Despite the numerous studies conducted on thin-walled energy absorbers, the simultaneous investigation of the effects of multiple geometric parameters on the performance of S-shaped absorbers, and the integration of finite element simulation, neural networks, and evolutionary algorithms within a unified optimization framework, still requires further attention. In particular, the simultaneous optimization of wall thickness, cross-sectional width, curvature radius, and curvature angle with the aim of achieving a balance between increasing absorbed energy and controlling the peak crushing force is of special importance. This problem is inherently multiobjective, because increasing energy absorption capacity is not necessarily accompanied by a reduction in peak crushing force, and achieving a desirable response requires trade-offs between conflicting design objectives.

Accordingly, in the present study, an integrated numerical and optimization framework is proposed for the multiobjective design of S-shaped thin-walled energy absorbers. In the first stage, the crushing behavior of the S-shaped absorber is simulated using the finite element method in ABAQUS software, and the numerical results are validated against experimental data available in reference [36]. Subsequently, using the results of the numerical simulations, a dataset is generated comprising various combinations of geometric parameters including wall thickness, cross-sectional width, curvature radius, and curvature angle. Next, an RBF neural network is employed to create a surrogate model and extract the nonlinear relationship between the geometric variables and the two main performance indicators, namely absorbed energy and peak crushing force. Finally, the DE algorithm is used to solve the multiobjective optimization problem and determine the set of non-dominated solutions, or Pareto front.

The main novelty of this research lies in presenting an integrated approach based on finite element modeling, RBF neural networks, and the DE algorithm for the simultaneous optimization of geometric parameters of the S-shaped absorber. This framework, while reducing the need for numerous expensive simulations, enables the systematic investigation of the effects of geometric parameters on absorber performance and identifies a set of optimal designs with an appropriate trade-off between absorbed energy and peak crushing force.

Ultimately, the performance of the obtained optimal designs is compared with the results reported in previous studies [37], and the capability of the proposed method in improving the performance of S-shaped energy absorbers is evaluated. For a more comprehensive investigation, the effect of internal reinforcements as well as the application of metal foams [37] will be addressed as complementary approaches in the Discussion of results. The use of advanced materials such as high-strength steels [38] and multi-material design [20] will also be briefly examined in the results analysis section as potential strategies for simultaneously improving energy absorption and weight reduction. Recent research in 2026 [34], [35] has also shown that inspiration from biological structures and the use of data-driven rapid assessment frameworks can open new horizons in the design of high-performance energy absorbers, which will be referred to in the final section of the paper.

2 | Numerical Modeling of the S-Shaped Energy Absorber

In order to study the mechanical behavior of the thin-walled S-shaped energy absorber subjected to axial loading and to produce the necessary data needed for subsequent surrogate model building and optimization processes, a 3D FE model of the absorber was developed using ABAQUS/explicit software. Using the FE method allows simulating large deformation, local buckling, progressive crushing, and plastic deformation of the absorber. Numerical simulation is more efficient than performing a considerable number of experiments on the subject of the absorber's crushing.

2.1|Geometry of the Energy Absorber

In this study, a thin-walled S-shaped absorber having its geometry described by a 3D model was used. Four geometric parameters such as cross-sectional width (C), wall thickness (t), radius of curvature (R), and curvature angle were selected as the main design variables. The total length of the absorber (L=1 m was fixed for all absorbers. Geometric description of the absorber and the geometric parameters used in this study are shown in *Fig. 1*.

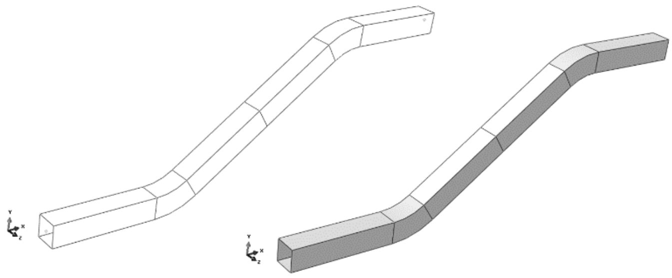

Fig. 1. Geometry of the thin-walled S-shaped energy absorber and the investigated geometric parameters.

The application of the axial loading was achieved by placing the absorber between two rigid plates. The upper rigid plate was taken as the fixed support, while the lower one played the role of an impactor. The general structure of the impact test system along with the S-shaped absorber is shown in *Fig. 2*.

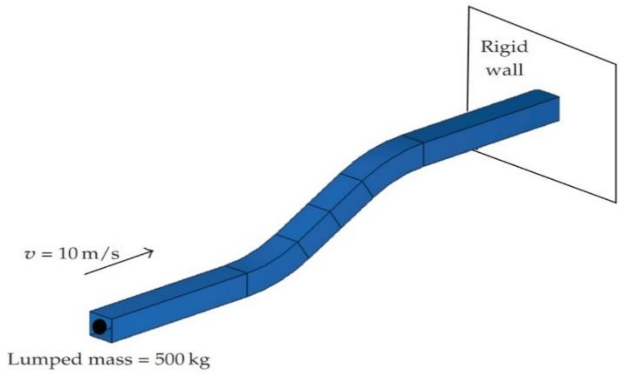

Fig. 2. Finite element model configuration of the S-shaped energy absorber and the applied axial loading.

2.2|Material Model

It was assumed that the energy absorber was made of steel. The elastic material characteristics, such as Young's modulus (E = 206 GPa), Poisson's ratio $\nu = 0.33$, and density $\varrho = 7800)\mathrm{kg/m^3}$, were introduced in the numerical model. The nonlinear plastic behavior of the material was described with the help of the Johnson-Cook constitutive model, which is used extensively for characterization of the material under large plastic deformations and dynamic loads.

$$\sigma = A + B\varepsilon_p^n, \quad (1)$$

where σ is the flow stress, ε_p is the equivalent plastic strain, and (A), (B), and (n) are the material-model parameters. The plastic stress-strain data that were adopted in the numerical analyses were based on the material data presented in [39].

2.3 | Contact and Boundary Conditions

In order to model the crushing process, both the contact behavior between the absorber and the rigid plates as well as self-contact between the various sections of the absorber during the crushing process were considered. The contact behavior between the absorber and the rigid plates was modeled through the surface-to-surface contact approach. Moreover, the self-contact option was taken into account to prevent any interpenetration among different parts of the structure.

The coefficient of friction between the absorber and the rigid plates was assumed to be 0.3 as suggested in Ref. [17]. The frictional behavior was represented through the penalty approach.

A concentrated mass of 500 kg was used to model the mass of the impactor. Then, an impactor velocity of 10 m/s was considered along the longitudinal axis of the absorber, where an initial velocity was applied to the lower plate. The upper rigid plate was restrained completely, while the lower plate was restrained from moving along the principal axis of the structure. Hence, the initial kinetic energy of the impactor was converted into plastic deformation and crushing of the S-shaped absorber.

2.4 | Finite Element Mesh

In order to reproduce the local deformation mode due to the thin-walled structure, the absorber was modeled using four-node S4R shell elements. This is because reduced-integration shell elements are appropriate for analyzing thin-walled structures under large deformation and plastic collapse. The mesh size was selected through a mesh independence study, where no substantial changes were obtained in the main responses of the structure (absorbed energy, maximum crushing force. The resulting finite element mesh used in the present simulations is shown in *Fig. 3*.

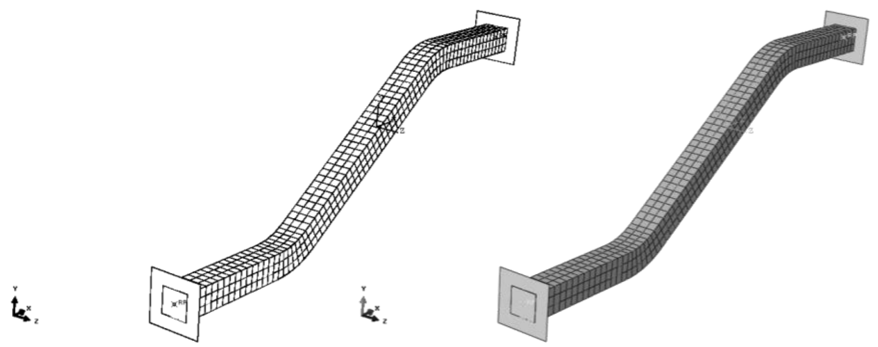

Fig. 3. Finite element mesh used for modeling the S-shaped energy absorber.

2.5 | Numerical Simulation of the Crushing Process

After establishing the geometric parameters, material properties, interaction between elements, boundary conditions, and meshing, an explicit dynamic simulation was conducted in ABAQUS/Explicit software. In the initial state of the simulation, the absorber was in its undeformed state, whereas the lower rigid plate was moving at a speed of 10 m/s. With the motion of the lower plate in the upward direction, the absorber experiences axial compression leading to plastic deformation.

The deformation consists of buckling initiation, folding, and crushing processes. The final deformed configuration of the absorber under axial loading is shown in *Fig. 4*. It is clear that the deformation behavior shows the ability of the developed numerical model to replicate the main crushing process of the S-shaped energy absorber.

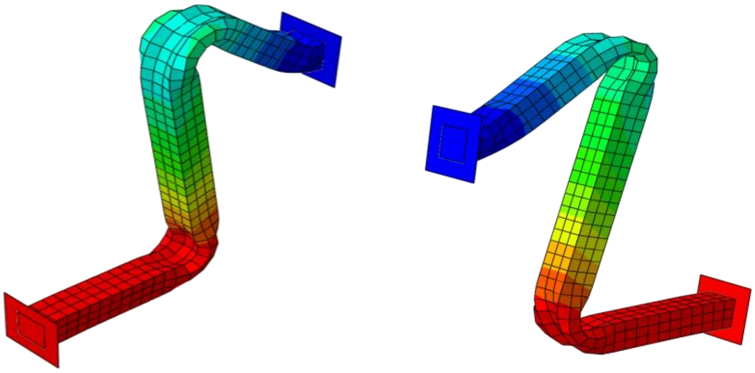

Fig. 4. Deformed configuration of the S-shaped energy absorber under axial loading and progressive crushing.

2.6 | Set of Numerical Models

In order to study the influence of the geometric parameters on the performance of the absorber and to create the dataset for surrogate modeling using neural networks, 58 different designs of the S-shaped energy absorber were numerically simulated. In the numerical simulations, four geometric parameters (C), (θ), (R), and (t) varied in the investigated ranges, while the other geometrical parameters and material properties remained unchanged.

The absorbed energy and peak crushing force of each configuration have been determined from the numerical data and used as output variables of the surrogate models and objective functions in the optimization process.

2.7 | Validation of the Finite Element Model

In order to verify the correctness of the created numerical model, its results have been compared with the results reported by Xu et al. [40]. For this purpose, 58 numerical models with different combinations of geometric parameters were created. Some of the obtained results were used for the training of the neural network, while the other part formed the independent testing dataset.

There was reasonable agreement between the results of the current finite element modeling and the reference values. The maximum difference between the two for the independent test data was 2.86% in terms of absorbed energy and 0.75% for the peak crushing force. Such reasonable differences suggest that the current finite element model offers adequate accuracy in the prediction of the crushing behavior of the S-shaped energy absorber.

For the purpose of comparing the current results with the reference values, *Fig. 5* shows the results of the absorbed energy and peak crushing force from the current modeling and the reference values. The closeness of the data points to the (y=x) line suggests reasonable agreement between the two sets of results.

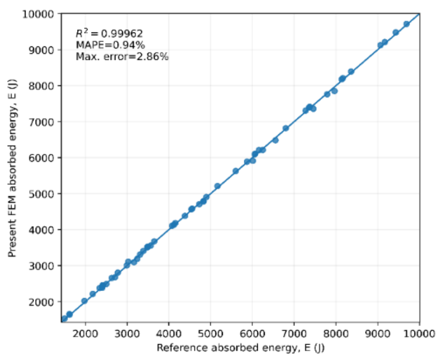

a.

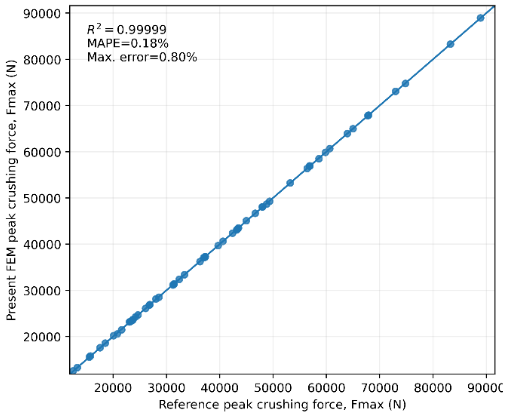

b.

Fig. 5. Comparison of the present finite element results with the reference results [27]; a. absorbed energy and b. peak crushing force.

Since the developed FEM model has proved to have satisfactory levels of accuracy after being validated, it is possible to use it as the main computational model for generating the required data. Such data was later used for developing the nonlinear relationship between the design parameters and performance characteristics of the absorber based on the RBF and Group Method of Data Handling (GMDH) models.

3 | Development and Evaluation of the GMDH Model for Predicting the Performance of an S-Shaped Energy Absorber

In order to reduce the computational cost of finite element analysis and predict the performance of the energy absorber rapidly, a surrogate model based on the GMDH neural network has been proposed. In the surrogate model, the geometric parameters of the energy absorber, such as C, θ, R, and t, are used as the input variables; meanwhile, two performance indicators, which are the absorbed energy (E_{abs}) and the peak crushing force (F_{max}), are taken as the output variables.

The database for the network development was generated from the finite element analysis results of 58 S-shaped energy absorbers. Among these absorbers, 49 were taken for the network training; meanwhile, 9 absorbers were chosen as independent samples for the evaluation of the model's prediction accuracy. The optimum structure of the GMDH network was determined using a genetic algorithm. Then, the prediction capability of the model was investigated by comparing the results of the GMDH network with those of finite element analysis.

3.1 | Predicting Absorbed Energy

The GMDH network was created first to predict the absorbed energy of the S-shaped energy absorber. The optimized architecture of the network is made up of a number of second-order polynomial functions that are used to capture the nonlinear interactions between the geometric input parameters and the absorbed energy. These equations corresponding to the network neurons were derived as follows:

$$
\begin{aligned}
y_1 &= 10000\begin{pmatrix} -1.207215 + 0.048957x_1 - 0.358609x_4 - \\ 0.000446x_1^2 + 0.076402x_4^2 + 0.005677x_1x_4 \end{pmatrix} \\
y_2 &= 1000\begin{pmatrix} 2.657371 + 0.001502x_3 - 2.409573x_4 - \\ 1.342\times10^{-6}x_3^2 + 1.156071x_4^2 + 0.000843x_3x_4 \end{pmatrix} \\
y_3 &= 10000\begin{pmatrix} 1.223103 - 0.044193x_2 - 0.000375x_3 + \\ 0.000520x_2^2 - 1.098\times10^{-7}x_3^2 + 0.00002607x_2x_3 \end{pmatrix} \\
y_4 &= 10000\begin{pmatrix} -1.091361 + 0.065236x_1 - 0.031937x_2 - \\ 0.000488x_1^2 + 0.000362x_2^2 + 0.00004266x_1x_2 \end{pmatrix}.
\end{aligned} \tag{2}
$$

In addition, the outputs of the intermediary neurons were then combined as follows:

$$
\begin{aligned}
y_5 &= \begin{pmatrix} 0.00017893 + 0.618805y_1 + 0.254887y_2 + \\ 0.00014485y_1^2 + 0.00014470y_2^2 - 0.00027354y_1y_2 \end{pmatrix} y_6 \\
&= \begin{pmatrix} 0.000003568 + 0.038247y_3 + 0.732736y_4 + \\ 0.00050152y_3^2 + 0.00051146y_4^2 - 0.00097897y_3y_4 \end{pmatrix}.
\end{aligned} \tag{3}
$$

The absorbed energy was finally predicted using the following equation:

$$
E_{abs} = \begin{pmatrix} -0.00001972 + 0.601432y_5 - 0.093318y_6 \\ -0.00003085y_5^2 + 0.000008186y_6^2 + 0.00012231y_5y \end{pmatrix}_6. \tag{4}
$$

The performance of the model can be estimated by comparing the absorbed energy values predicted using the GMDH network and those obtained from the finite element analysis. Figure 6 shows the scatter diagrams of the absorbed energy values.

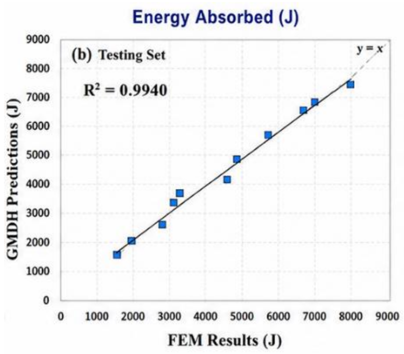

a.

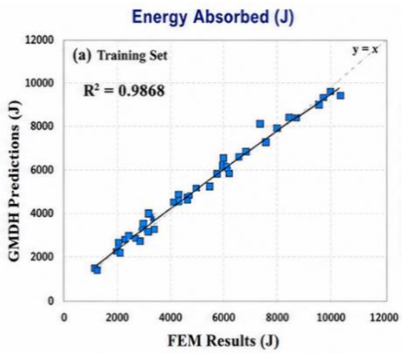

b.

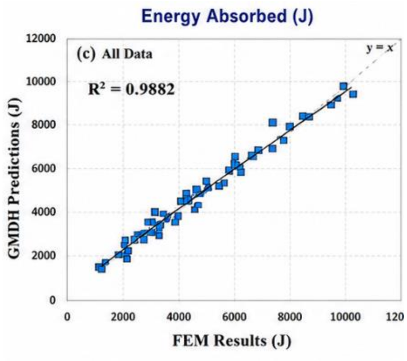

c.

Fig. 6. Comparison between FEM results and GMDH predictions for absorbed energy; a. training data, b. testing data, and c. overall dataset.

As shown in *Fig. 6a*, the data points corresponding to the training dataset are closely distributed around the ideal line, yielding a coefficient of determination of R2 = 0.9868. The high R2 value demonstrates that the GMDH network has a very good capability to learn the nonlinear relationship between the geometric parameters of the energy absorber and the absorbed energy.

The generalization capability of the developed model was evaluated using an independent testing dataset. As shown in *Fig. 6b*, the coefficient of determination for the testing dataset was ($R^2 = 0.9940$). The close agreement between the predicted data points and the fitting line, together with the high (R^2) value, indicates that the model maintains excellent predictive performance even for data that were not used during the training process.

Finally, the simultaneous comparison of all training and testing data in *Fig. 6c* resulted in an overall coefficient of determination of ($R^2 = 0.9882$). Therefore, the small discrepancies between the FEM and GMDH results demonstrate that the developed surrogate model can accurately reproduce the absorbed-energy behavior of the S-shaped energy absorber.

3.2 | Prediction of the Maximum Crushing Force

In the next step, the GMDH model was developed to predict the maximum crushing force of the S-shaped energy absorber. This parameter is of particular importance in the design of energy absorbers because an excessively high crushing force can result in severe load transfer to the protected structure or occupant. Therefore, accurate prediction of (F_{max}) is essential for the design and optimization of the energy absorber.

The optimized GMDH network structure for predicting the maximum crushing force was composed of the following quadratic polynomial relationships:

$$\begin{aligned}
y_1 &= 10000\begin{pmatrix}5.750596 - 0.145030x_2 - 0.000449x_3 + \\ 0.001025x_2^2 - 2.205\times10^{-6}x_3^2 + 0.000241x_2x_3\end{pmatrix} \\
y_2 &= 1000\begin{pmatrix}-6.866123 + 0.039342x_3 + 4.338069x_4 - \\ 0.00002950x_3^2 + 3.260853x_4^2 + 0.010015x_3x_4\end{pmatrix} \\
y_3 &= \begin{pmatrix}-0.0002125 + 1.044552y_1 - 0.022386x_2 - \\ 0.000001674y_1^2 - 1.719680x_2^2 + 0.002496y_1x_2\end{pmatrix} \\
y_4 &= \begin{pmatrix}-0.00009523 - 0.164273y_2 - 0.006509x_1 - \\ 0.000000488y_2^2 - 0.446169x_1^2 + 0.020414y_2x_1\end{pmatrix}.
\end{aligned} \tag{5}$$

Finally, the maximum crushing force was calculated from the following expression:

$$\mathrm{F}\begin{pmatrix}0.00002157 + 0.432650\mathrm{y}_3 + 0.6549997\mathrm{y}_4 - \\ 0.000011582\mathrm{y}_3^2 - 0.000001645\mathrm{y}_4^2 + 0.000011499\mathrm{y}_3\mathrm{y}_4\end{pmatrix}_{\max}. \quad (6)$$

The performance of the developed GMDH model in predicting the maximum crushing force is presented in *Fig. 7*.

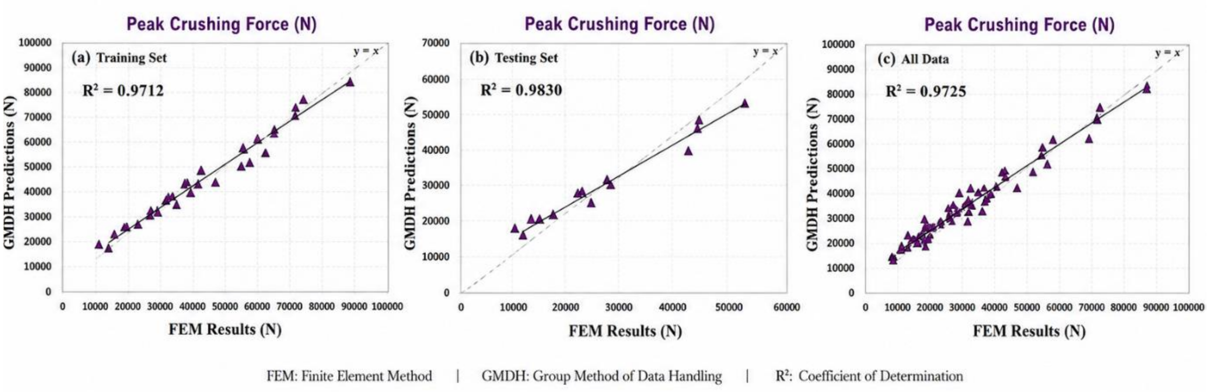

Fig. 7. Comparison between FEM results and GMDH predictions for the maximum crushing force; a. training data, b. testing data, and c. the complete dataset.

As can be observed in *Fig. 7a*, the predicted data points for the training dataset are very close to the trend line of FEM results, with a coefficient of determination of (R^2=0.9712). The relatively high value of (R^2) represents the strong relationship between the results obtained by the GMDH model and the numerical results, which indicates the effectiveness of the established model in capturing the nonlinear relationship between geometric parameters and maximum crushing force.

For the testing dataset that is independent of the training dataset, as illustrated in *Fig. 7b*, the coefficient of determination is increased to (R^2=0.9830).

The coefficient of determination (R^2=0.9725) for the entire dataset, consisting of both training and testing samples, is R^2=0.9725 and is illustrated in *Fig. 7c*. Even though there is some scatter in the data points, which is more significant compared to the absorbed energy model, the GMDH model captures the general trend of the finite element method solution. The relatively higher scatter in the data points is because the maximum crushing force is a rather complex parameter depending on several factors, including the point of crushing initiation, development of plastic folds, and geometrical changes occurring during the progressive collapse of the S-shaped structure.

Overall, it is confirmed that the developed GMDH-based surrogate model is an effective computational tool for predicting the maximum crushing force of the S-shaped thin-walled energy absorbers. The high correlation between the data points in both training and testing datasets further confirms the applicability of the model for multiobjective optimization.

3.3 | Comparison and Discussion of the Performance of the GMDH Models

For the purpose of comparing the performance of both models, the values of the coefficients of determination (R^2) calculated from training, testing, and total datasets are tabulated below.

The data clearly show that both models possess high accuracy in prediction. Nevertheless, the GMDH model proves more effective in predicting the absorbed energy compared to the maximum crushing force. The maximum value of (R^2) is calculated for the testing dataset of the absorbed-energy model as (R^2 = 0.9940).

Table 1. Comparison of the GMDH model performance for predicting the absorbed energy and maximum crushing force of the S-shaped energy absorber.

Objective Function	Training R^2	Testing R^2	Complete Dataset R^2
Absorbed energy	0.9868	0.9940	0.9882
Maximum crushing force	0.9712	0.9830	0.9725

However, the value of (R^2=0.9830) achieved for the test dataset of the maximum crushing force also indicates the high prediction accuracy of the proposed neural network model. The reason for the discrepancy in the performance of the two models is due to the difference in the nature of these two response variables. The absorbed energy is a cumulative quantity based on the overall deformation of the structure and, therefore, behaves in a relatively smooth way. On the other hand, the maximum crushing force is a local response that depends heavily on the first fold formation and local buckling.

4 | Multiobjective Optimization of the S-Shaped Energy Absorber

Based on the results obtained from the finite element analysis and data-driven modeling, a multiobjective optimization of the S-shaped energy absorber was performed to simultaneously achieve a high energy absorption capacity and a low maximum crushing force. Owing to the conflicting nature of these two performance criteria, achieving the optimum value of both objective functions simultaneously is not possible. Therefore, the problem was formulated as a multiobjective optimization problem based on the concept of the Pareto front.

In this optimization problem, four geometric parameters, namely the parameter (C), angle (\theta), radius (R), and wall thickness (t), were considered as the design variables. Accordingly, the design-variable vector was defined as follows:

$$X = [C, \theta, R, t]. \tag{7}$$

The ranges of the design variables were determined according to the ranges considered in the numerical models. The remaining geometric parameters and loading conditions, including the structure diameter (D = 150 mm), structure length (L = 1 m), impactor mass (500 kg), and initial velocity (10 m/s), were kept constant.

4.1 | Formulation of the Multiobjective Optimization Problem

For the optimal design of the S-shaped energy absorbers, a bi-objective optimization problem was formulated considering the aforementioned design parameters. The mathematical polynomial models obtained from the GMDH and RBF modeling presented in the previous section were employed as surrogate models for the multiobjective optimization process. Based on these mathematical relationships, the optimization procedure was performed without the need to conduct computationally expensive finite element simulations repeatedly.

One of the most important requirements in the optimal design of energy absorbers is to increase the energy absorption capability while simultaneously reducing the maximum crushing force. An energy absorber can be considered to have a desirable design when it is capable of absorbing a large amount of energy while maintaining a relatively low maximum crushing force. Conversely, a design that absorbs a large amount of energy but generates an excessively high crushing force is not considered optimal. Similarly, an energy absorber with a low crushing force but insufficient energy absorption capacity cannot be regarded as a desirable design.

Accordingly, the absorbed energy (E_{abs}) and the maximum crushing force (F_{max}) were considered as two conflicting objective functions in the present optimization problem. The objective was therefore to maximize the absorbed energy while simultaneously minimizing the maximum crushing force. The multiobjective optimization problem can consequently be formulated as follows:

$$\text{Maximize} \quad f_1 = E(\theta, R, C, t) \text{ (Absorbed Energy)} \tag{8}$$

$$\text{Minimize} \quad f_2 = F(\theta,)(\text{ R, C, t Peak Crushing Force})$$

$$R \leq \frac{D}{2(1 - \text{Cos}\theta)},$$

where (C), (θ), (R), and (t) represent the geometric design variables of the S-shaped energy absorber. The resulting set of non-dominated solutions represents the Pareto-optimal front, from which an appropriate design can be selected according to the desired balance between energy absorption capacity and crushing-force level.

4.2 | Multiobjective Optimization Algorithm

The DE approach was used to solve the above-stated optimization problem. The DE approach starts with the generation of an initial population of solutions within the design space and develops this population through successive generations. In each generation, trial vectors are created through the application of the mutation and crossover processes and then compared to the existing solutions.

As far as the multiobjective problem formulation is concerned, the solution selection is done according to the principle of non-dominance. Thus, the solutions that are not dominated by other solutions concerning the two objective functions are selected. Moreover, the crowding distance approach is used to avoid the overcrowding of certain parts of the Pareto front with solutions and maintain diversity among the non-dominated solutions.

In the current case, the initial population size was equal to 100, the maximum number of generations was 500, the mutation factor equaled 0.1, and the crossover rate was 0.8. The process of evolution was carried out until the predefined number of generations was achieved. Finally, the set of non-dominated solutions was obtained as the solution to the multiobjective optimization problem.

4.3 | Results of the Multiobjective Optimization

Eight non-dominated optimal solutions were obtained in the process of optimization, as illustrated in the relevant figure. All of them could be regarded as alternative optimal designs, and the final choice depends on particular design requirements.

One can see that improving the value of one objective function leads to the degradation of the value of another objective function. It means that there exists some trade-off between the two objective functions. From among the Pareto-optimal solutions, Point A is characterized by minimum absorbed energy and minimum maximum crushing force. At the same time, Point B corresponds to maximum absorbed energy but higher maximum crushing force. Thus, neither of them could be considered the most appropriate solution.

Taking into account that the primary design aims to find the right balance between energy absorption and limitation of the crushing force, Point C was chosen as the most preferable compromise solution. The value of absorbed energy at Point C is approximately 33,400 J, and the maximum crushing force is about 8,713 N. The geometric design parameters are as follows:

$$[x_1 = 50, \quad x_2 = 45, \quad x_3 = 1284, \quad x_4 = 2.59]. \tag{9}$$

Fig. 8 illustrates the Pareto front achieved using the multiobjective optimization procedure. As seen in the figure, the movement along the Pareto front towards higher absorbed energy is accompanied by an increase in the maximum crushing force. Such a tendency demonstrates the existence of an intrinsic trade-off between the two objective functions; that is, the increase in the capacity for energy absorption is usually associated with an increased crushing force.

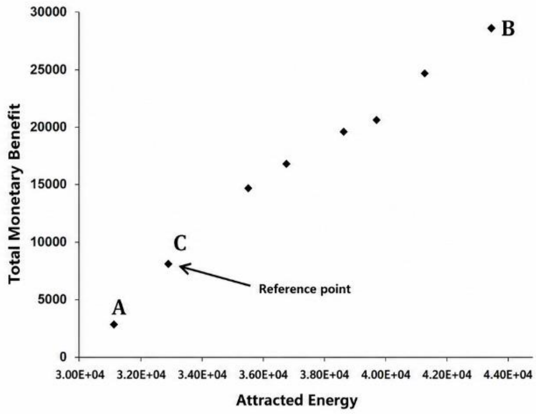

Fig. 8. Pareto front obtained from the multiobjective optimization of the S-shaped energy absorber based on absorbed energy and maximum crushing force.

Of all the Pareto solutions, Point A corresponds to the lower performance area of the Pareto front in terms of both absorbed energy and crushing force. At the same time, Point B lies in the area of maximal capacity of energy absorption with the increase in the maximum crushing force. Consequently, none of these points can be considered the best design option.

In accordance with the primary purpose of obtaining a proper balance between energy absorption and crushing-force minimization, Point C was chosen as the best compromise solution. It offers an absorbed energy value of approximately 33,400 J and the maximum crushing force of approximately 8,713 N. The geometric parameters of the chosen optimal design are:

$$\mathrm{C} = 50; \mathrm{mm}, \theta = 45^{\circ}, \mathrm{R} = 1284; \mathrm{mm}, \mathrm{t} = 2.59; \mathrm{mm}. \quad \textbf{(10)}$$

The above results clearly show that the joint use of the GMDH surrogate model and DE algorithm allows for an effective exploration of the design space of the S-shaped energy absorber by using significantly fewer computations than a large number of finite element simulations. In addition, the proposed methodology allows for obtaining a set of non-dominated solutions that enables the designer to choose a design depending on the desirable compromise between energy absorption and crushing force.

4.4 | Comparison of the Optimization Results with Reference Data

To assess the effectiveness of the obtained designs, the Pareto-optimal solutions were compared with the data for the reference specimens. The results of the comparison are shown in *Fig. 9*.

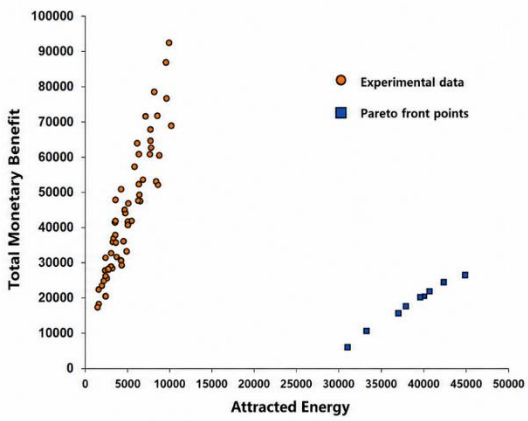

Fig. 9. Comparison of the obtained Pareto-optimal solutions with the reference data.

As can be seen from *Fig. 7*, the designs obtained through the optimization are located in a performance region providing a good trade-off between absorbed energy and maximum crushing force. Thus, it can be said that the proposed methodology is able to find the promising design regions and to generate competitive designs compared with the reference specimens.

Last but not least, since it is a multiobjective problem, there is no absolute best solution. Hence, the optimal choice can only be made based on the design criteria set. Point C, in this case, is chosen as the optimal design for the reason that it makes a perfect balance between maximizing energy absorption and minimizing the peak crushing load.

5 | Conclusion

This research work has introduced a coupled approach of numerical and data-driven techniques for the multiobjective optimization of the thin-walled S-shaped energy absorbers under axial impact loading. In order to have a proper balance between the absorbed energy and peak crushing force, the approach involves finite element modeling, artificial neural network-based surrogate modeling, and the application of the DE algorithm. Three-dimensional finite element modeling has been done using ABAQUS/Explicit software for simulating the process of gradual crushing of the S-shaped absorber. The results obtained numerically agreed well with the data, with a maximum difference of 2.86% and 0.75% for absorbed energy and peak crushing force, respectively. This indicates the validity of the finite element model used for creating the database for surrogate modeling and optimization.

With the help of the results of 58 FE simulations, surrogate models based on RBF and GMDH neural networks were created to describe the nonlinear connection between the key geometric dimensions and the crashworthiness responses. The GMDH model showed good performance with determination coefficients of 0.9882 for the absorbed energy and 0.9725 for the peak crushing force. This is because the peak crushing force is much more localized and nonlinear, which means that the prediction of its value is greatly influenced by the beginning of crushing, local buckling, and progressive plastic folding. Next, the surrogate models were used in a multiobjective optimization scheme using the DE algorithm. As a result, the set of non-dominated solutions was obtained. There was a conflict between the two objectives, meaning that any increase in the absorbed energy was usually associated with the growth of the peak crushing force. Thus, the Pareto front gives us a number of alternatives from which we can choose the most appropriate one. Of the Pareto optimal solutions found, Point C is considered to be a good compromise solution with respect to energy absorption and peak crushing force. Such a design was able to provide an absorbed energy of approximately 33,400 J and a peak crushing force of approximately 8,713 N. In general, it can be concluded that the proposed method based on FEA simulation, RBF/GMDH models, and the DE algorithm is capable of offering an effective way for the crashworthiness optimization of S-shape energy absorbers. It allows one to reduce the number of expensive FEA simulations significantly and explore the design space efficiently.

Conflict of Interest

The authors declare that there are no conflicts of interest regarding the publication of this paper.

Data Availability

The datasets generated and/or analyzed during the current study are included in this article.

Funding

This study was carried out without any specific funding from public, commercial, or non-profit organizations.

Reference

[1] Abramowicz, W., & Jones, N. (1984). Dynamic axial crushing of square tubes. *International journal of impact engineering*, *2*(2), 179–208. https://doi.org/10.1016/0734-743X(84)90005-8

[2] Wierzbicki, T., & Akerstrom, T. (1977). Dynamic crushing of strain rate sensitive box columns. *Second international conference on vehicle structural mechanics, southfield, michigan*. SAE International. https://doi.org/10.4271/770592

[3] Redwood, R. C. (1964). On the buckling of thin-walled tubes under axial impact. *The journal of the royal aeronautical society*, *68*(642), 418–419. https://doi.org/10.1017/S0368393100079633

[4] Yamazaki, K., & Han, J. (1998). Maximization of the crushing energy absorption of tubes. *Structural Optimization*, *16*(1), 37–46. https://doi.org/10.1007/BF01213998

[5] Nariman-zadeh, N., Darvizeh, A., & Jamali, A. (2006). Pareto optimization of energy absorption of square aluminium columns using multiobjective genetic algorithms. *Proceedings of the institution of mechanical engineers, part b: Journal of engineering manufacture*, *220*(2), 213–224. https://doi.org/10.1243/095440506X78156

[6] Zhang, Y., Sun, G., Li, G., Luo, Z., & Li, Q. (2012). Optimization of foam-filled bitubal structures for crashworthiness criteria. *Materials & Design*, *38*, 99–109. https://doi.org/10.1016/j.matdes.2012.01.028

[7] Zarei, H., & Kröger, M. (2008). Optimum honeycomb-filled crash absorber design. *Materials & Design*, *29*(1), 193–204. https://doi.org/10.1016/j.matdes.2006.10.013

[8] Zarei, H. R., & Kröger, M. (2008). Optimization of the foam-filled aluminum tubes for crush box application. *Thin-walled structures*, *46*(2), 214–221. https://doi.org/10.1016/j.tws.2007.07.016

[9] Ohkami, Y., Shimamura, M., Takada, K., Tomizawa, H., Motomura, K., & Usuda, M. (1990). Collapse of thin-walled curved beam with closed-hat section – part 1: Study on collapse characteristics. *SAE Transactions*, *99*, 604–615. https://doi.org/10.4271/900460

[10] Liu, Y., & Day, M. L. (2008). Bending collapse of thin-walled circular tubes and computational application. *Thin-walled structures*, *46*(4), 442–450. https://doi.org/10.1016/j.tws.2007.07.014

[11] Kim, H. S., & Wierzbicki, T. (2001). Effect of the cross-sectional shape on crash behaviour of a three-dimensional space frame. *International journal of vehicle design*, *25*(4), 295–316. https://doi.org/10.1504/IJVD.2001.005204

[12] Kim, H. S., & Wierzbicki, T. (2001). Effect of the cross-sectional shape of hat-type cross-sections on crash resistance of an "S"-frame. *Thin-walled structures*, *39*(7), 535–554. https://doi.org/10.1016/S0263-8231(01)00020-9

[13] Zheng, L., & Wierzbicki, T. (2004). Quasi-static crushing of S-shaped aluminum front rail. *International journal of crashworthiness*, *9*(2), 155–173. https://doi.org/10.1533/ijcr.2004.0284

[14] Zhang, C., & Saigal, A. (2007). Crash behavior of a 3D S-shape space frame structure. *Journal of Materials Processing Technology*, *191*(1), 256–259. https://doi.org/10.1016/j.jmatprotec.2007.03.093

[15] Esmaeili-Marzdashti, S., Pirmohammad, S., & Esmaeili-Marzdashti, S. (2017). Crashworthiness analysis of S-shaped structures under axial impact loading. *Latin american journal of solids and structures*, *14*(5), 743–764. https://doi.org/10.1590/1679-78253430

[16] Soheili, E., & Feli, S. (2024). Grooves and cross-section effects on energy absorption of S-shaped tubes under axial quasi-static and impact loading. *Journal of the institution of engineers (india): series c*, *105*(1), 215–232. https://doi.org/10.1007/s40032-023-01010-2

[17] Han, J., & Yamazaki, K. (2003). Crashworthiness optimisation of S-shape square tubes. *International journal of vehicle design*, *31*(1), 72–85. https://doi.org/10.1504/IJVD.2003.002048

[18] Liu, S. T., Tong, Z. Q., Tang, Z. L., & Zhang, Z. H. (2014). Design optimization of the S-frame to improve crashworthiness. *Acta Mechanica Sinica*, *30*(4), 589–599. https://doi.org/10.1007/s10409-014-0032-y

[19] Nguyen, V. S., Wen, G., Yin, H., & Van, T. P. (2014). Optimisation design of reinforced S-shaped frame structure under axial dynamic loading. *International journal of crashworthiness*, *19*(4), 385–393. https://doi.org/10.1080/13588265.2014.904598

[20] Hosseini-Tehrani, P., & Nikahd, M. (2006). Two-material S-frame representation for improving crashworthiness and lightening. *Thin-walled structures*, *44*(4), 407–414. https://doi.org/10.1016/j.tws.2006.04.002

[21] Pyrz, M., & Krzywoblocki, M. (2019). Crashworthiness optimization of front rail structure using macro element method and evolutionary algorithm. *Structural and Multidisciplinary Optimization*, *60*(2), 711–726. https://doi.org/10.1007/s00158-019-02233-7

[22] Khakhali, A., Nariman-zadeh, N., Darvizeh, A., Masoumi, A., & Notghi, B. (2010). Reliability-based robust multiobjective crashworthiness optimisation of S-shaped box beams with parametric uncertainties. *International journal of crashworthiness*, *15*(4), 443–456. https://doi.org/10.1080/13588261003696458

[23] Yao, S., Zhou, Y., Xing, J., Xu, P., Huang, Q., & Zou, F. (2024). A crashworthiness optimization method of subway underframe structures based on the differential evolution of the weighted graph representation. *Structural and Multidisciplinary Optimization*, *67*(4), 62. https://doi.org/10.1007/s00158-024-03780-4

[24] Zhang, X., & Zhang, H. (2016). Crush resistance of square tubes with various thickness configurations. *International journal of mechanical sciences*, *107*, 58–68. https://doi.org/10.1016/j.ijmecsci.2016.01.003

[25] Marzbanrad, J., Alijanpour, M., & Kiasat, M. S. (2009). Design and analysis of an automotive bumper beam in low-speed frontal crashes. *Thin-walled structures*, *47*(8), 902–911. https://doi.org/10.1016/j.tws.2009.02.007

[26] Sun, G., Li, G., Zhou, S., Li, H., Hou, S., & Li, Q. (2011). Crashworthiness design of a vehicle using multiobjective robust optimization. *Structural and Multidisciplinary Optimization*, *44*(1), 99–110. https://doi.org/10.1007/s00158-010-0601-z

[27] Fang, J., Gao, Y., Sun, G., Xu, C., & Li, Q. (2015). Multiobjective robust design optimization of fatigue life for a truck cab. *Reliability engineering & system safety*, *135*, 1–8. https://doi.org/10.1016/j.ress.2014.10.007

[28] Acar, E., Guler, M. A., Gerçeker, B., Cerit, M. E., & Bayram, B. (2011). Multiobjective crashworthiness optimization of tapered thin-walled tubes with axisymmetric indentations. *Thin-walled structures*, *49*(1), 94–105. https://doi.org/10.1016/j.tws.2010.08.010

[29] Homsnit, T., Jongpradist, P., Kongwat, S., Jongpradist, P., & Thongchom, C. (2024). Crashworthiness design of an automotive S-rail using ANN-based optimization to enhance performance and safety. *Structural and Multidisciplinary Optimization*, *67*(6), 93. https://doi.org/10.1007/s00158-024-03803-0

[30] Gao, D., Li, Q., Liu, Z., & Chang, G. (2024). An active learning approach for multiobjective optimization and its application to the crashworthiness design of thin-walled structures. *Optimization and Engineering*, *25*(2), 699–730. https://doi.org/10.1007/s11081-023-09821-z

[31] Lian, F., Wang, D., Zhang, Z., Chen, H., & Xu, W. (2025). Multiobjective optimization of lightweight and crashworthiness of automotive front-end structures based on stacked regression surrogate. *Engineering applications of artificial intelligence*, *155*, 111138. https://doi.org/10.1016/j.engappai.2025.111138

[32] Xing, J., Xu, T., Xu, P., & Yao, S. (2025). Multi-dimensional crashworthiness performance prediction and constrained optimization of the HFC energy-absorbing structures for railway vehicles driven by deep learning frameworks. *Engineering Structures*, *338*, 120603. https://doi.org/10.1016/j.engstruct.2025.120603

[33] You, J., Zhao, Y., Jia, L., Wang, N., Sun, Z., Zou, W., … & Zhang, C. (2026). A fast crashworthiness assessment framework: Sectional force-based multi-stage physics-informed surrogate model. *Advances in Engineering Software*, *213*, 104090. https://doi.org/10.1016/j.advengsoft.2025.104090

[34] Van, H. T. (2026). Deformation behavior and energy absorption performance of thin-walled tube structures for automotive crash boxes. *Thu dau mot university journal of science*, *8*(2), 249–263. https://doi.org/10.37550/tdmu.ejs%2F2026.02.730

[35] Saber, A., Amer, A. M., Abd_Elsalam, A., Shehata, A. I., & El-Gamal, H. A. (2026). Design and optimization of a bio-inspired crash box based on seashell structure for enhanced crashworthiness. *Results in Engineering*, *32*, 111724. https://doi.org/10.1016/j.rineng.2026.111724

[36] Hosseinipour, S. J., & Daneshi, G. H. (2004). Experimental studies on thin-walled grooved tubes under axial compression. *Experimental Mechanics*, *44*(1), 101–108. https://doi.org/10.1007/BF02427984

[37] Khalkhali, A., & Samareh, M. S. (2012). Multiobjective crashworthiness optimization of the aluminum foam-filled tubes. *International journal of automotive engineering*, *2*(3), 180–193. https://scispace.com/pdf/multi-objective-crashworthiness-optimization-of-the-aluminum-kzm63tzmcz.pdf

[38] Li, Y., Lin, Z., Jiang, A., & Chen, G. (2003). Use of high-strength steel sheet for lightweight and crashworthy car body. *Materials & Design*, *24*(3), 177–182. https://doi.org/10.1016/S0261-3069(03)00021-9

[39] Hartman, E. J., Keeler, J. D., & Kowalski, J. M. (1990). Layered neural networks with Gaussian hidden units as universal approximations. *Neural Computation*, *2*(2), 210–215. https://doi.org/10.1162/neco.1990.2.2.210

[40] Xu, X., Jiang, Y., & Lee, H. P. (2017). Multiobjective optimal design of sandwich panels using a genetic algorithm. *Engineering Optimization*, *49*(10), 1665–1684. https://doi.org/10.1080/0305215X.2016.1265304